ELSEVIER

Biochimica et Biophysica Acta 1235 (1995) 419–427

BBA Biochimica et Biophysica Acta

Lateral domain formation in mixed monolayers containing cholesterol and dipalmitoylphosphatidylcholine or *N*-palmitoylsphingomyelin

J. Peter Slotte *

Department of Biochemistry and Pharmacy, Åbo Akademi University, FIN-20520 Turku, Finland

Received 13 September 1994; revised 29 November 1994; accepted 16 December 1994

Abstract

Epifluorescence microscopy was used to visualize the formation of lateral fluid domains in monolayers of dipalmitoylphosphatidylcholine (DPPC) or *N*-palmitoylsphingomyelin (*N*-P-SM) containing cholesterol. NBD-Cholesterol was used as a fluorophore at 1 mol%. Image analysis of the monolayer surface texture (taken during the first compression at 22° C and 1.5 mN/m) showed that the area of the liquid-condensed domains increased (from zero to 90% of the total area) with increasing cholesterol concentration (5 to 40 mol%), both in DPPC and *N*-P-SM mixed monolayers. The liquid-condensed domains had a significantly larger size in DPPC than in *N*-P-SM monolayers, but were more numerous in *N*-P-SM monolayers. Lateral domain boundary lines begun to dissipate at a certain surface pressure. This characteristic phase transformation pressure was markedly higher in *N*-P-SM (3–12 mN/m) than in DPPC mixed monolayers (1.8–3.7 mN/m), and also increased with increasing cholesterol concentration. If a monolayer was first compressed above the phase transformation pressure (to 15 mN/m), and then expanded to a lateral surface pressure of 1.5 mN/m, the liquid-condensed domains coalesced if the cholesterol concentrations was 25 mol% or higher (both DPPC and *N*-P-SM monolayers). In conclusion, the cholesterol/DPPC and cholesterol/*N*-P-SM interactions in the monolayers appeared to differ to a large extent, since the liquid-condensed domains in the two systems differed in number, size, and properties. Differences in molecular properties were reflected in the phase transformation pressures, which were markedly higher in cholesterol/*N*-P-SM monolayers as compared to cholesterol/DPPC membranes.

Keywords: Lateral domain; Phase separation; Cholesterol; Phosphatidylcholine; Sphingomyelin; Epifluorescence microscopy; Monolayer membrane

1. Introduction

Phosphatidylcholines and sphingomyelins constitute a major fraction of the phospholipids in the outer leaflet of cellular plasma membranes. In addition, cholesterol is known to be preferentially located in the plasma membrane compartment of many cell types [1–3]. In the membranes, cholesterol interacts with the phospholipids, thereby affecting their physico-chemical and structural properties [4]. The specific hydrophobic interaction between cholesterol and phospholipids is of major importance for the proper functioning of the plasma membrane as a fluid environment for membrane-bound metabolic processes [5].

Many lines of evidence suggest that the strength or mode of interaction of cholesterol with phosphatidylcholines and sphingomyelins differ. First, the molecular packing properties in cholesterol/sphingomyelin membranes have been suggested to differ from the corresponding cholesterol/phosphatidylcholine model membranes [6], although a recent report contradicts this suggestion [7]. It has also been reported that the water permeability is lower in sphingomyelin/cholesterol bilayer membranes than it is in phosphatidylcholine/cholesterol membranes [8,9], a finding which would be consistent with a tighter packing density in sphingomyelin containing membranes. In addition, it has been established that cholesterol desorption is markedly reduced from a sphingomyelin membrane as compared with a phosphatidylcholine membrane with similar acyl chain composition [6,10], a result which probably can be explained by increased opportunities for the formation of van der Waal's forces between cholesterol and sphingomyelin. Also, the compressibility modulus is re-

Abbreviations: DPPC, L-α-1,2-dipalmitoyl-*sn*-glycero-3-phosphocholine; *N*-P-SM, *N*-palmitoylsphingomyelin; NBD-cholesterol, 22-(*N*-(7-nitrobenz-2-oxa-1,3-diazol-4-yl)amino)-23,24-bisnor-5-cholen-3-ol.

* Corresponding author. Fax: +358 21 2654745.

SSDI 0005-2736(94)00325-4

ported to be twice as large in cholesterol/sphingomyelin membranes as it is in a 1-stearoyl-2-oleoyl-*sn*-glycero-3-phosphocholine/cholesterol bilayer [11]. Finally, using cholesterol oxidase to probe the strength of interaction between cholesterol and sphingomyelin or phosphatidylcholine, it was observed that the oxidation susceptibility of cholesterol was much reduced in a sphingomyelin monolayer as compared to a phosphatidylcholine system [12,13]. This suggested that cholesterol associated more strongly with sphingomyelin than with phosphatidylcholine, even though both phospholipids had comparable acyl chain compositions. Based on these and other results, it is clear that differences exist between phosphatidylcholines and sphingomyelins with regard to how they associate with cholesterol in membranes.

Recent advances in microscopic analysis of monolayer membranes at the gas/water interface have made it possible to visualize lateral domain formation in pure and mixed lipid monolayers [14–17]. Analysis of domain formation in mixed cholesterol/dimyristoylphosphatidylcholine and dipalmitoylphosphatidylcholine monolayers has been reported [18,19], but no information appears to be available about domain formation in cholesterol/sphingomyelin monolayer membranes. In this study, I have analyzed the formation of lateral domains in monolayers prepared from cholesterol and dipalmitoylphosphatidylcholine (DPPC) or cholesterol and *N*-palmitoylsphingomyelin (*N*-P-SM). The goal of this work was to compare the interaction of cholesterol with these two phospholipids at different cholesterol concentrations, and to characterize the lateral domains formed as a result of the molecular associations.

2. Experimental procedures

2.1. Materials

Cholesterol, DPPC, and *N*-P-SM were obtained from Sigma (St. Louis, MO, USA). Gas chromatographic analysis of cholesterol indicated that it was at least 99% pure. DPPC and *N*-P-SM gave a single spot when analyzed by thin-layer chromatography. These lipids were used as delivered. NBD-cholesterol was purchased from Molecular Probes (Eugene, OR, USA). With thin-layer chromatography, NBD-cholesterol showed only one spot and was therefore considered pure enough for use as delivered. The water used as subphase was purified by reverse osmosis followed by passage through a Millipore UF Plus water purification system, to yield a product with a resistivity better than 18 MΩ/cm.

2.2. Formation of monolayer at the air / water interface

The equipment used for the visualization of monolayers consisted of a KSV Minisystems surface barostat which could be mounted on the stage of an Olympus IMT-2 inverted epifluorescence microscope. The barostat performed symmetric compression of the monolayer (i.e., with two barriers from each end of the tough), and the trough (24 111 mm^2 area) was equipped with a 50 mm diameter quartz window in the center, which allowed for excitation and observation of the monolayer fluorophores. 30 nmol of lipids were spread from a hexane/2-propanol stock solution on pure water to form mixed monolayers at 22° C. The available molecular area at film spreading was 133.51 Å^2. These monolayers contained varying amounts of cholesterol and DPPC or *N*-P-SM, together with 1 mol% NBD-cholesterol. After application, the monolayers were compressed symmetrically at a speed of 3.4 Å^2/molecule, min to a lateral surface pressure of 1.5 mN/m. At this lateral compression, the monolayers were observed with epifluorescence microscopy, and documented using a Hitachi video camera connected to a DT3851 digitizing board (Data Translation, Marlboro, MA, USA). Mixed monolayers were also compressed beyond the characteristic phase transformation pressure (to 15 mN/m). The monolayer was kept at 15 mN/m for 30 s after which it was allowed to expand back to 1.5 mN/m (the compression and expansion barrier speed was identical), at which point a new documentation was undertaken.

2.3. Analysis of monolayers

The quantification of domain size (area) and number was performed on the digitized images using Image Pro plus (v. 1.2) or Global Lab Image (v. 2.2) software.

3. Results

3.1. Surface texture of mixed monolayers

The lateral phase partitioning properties of NBD-cholesterol has previously been shown to be similar to that of *sn*-2 acyl chain labeled NBD-phosphatidylcholine [20]. Both NBD-cholesterol [20] and NBD-phosphatidylcholine [17,21] partition preferentially into loosely packed liquid-

Fig. 1. Domain formation as a function of cholesterol concentration. Mixed monolayers containing increasing amounts of cholesterol (from 5 to 40 mol%) were prepared with either DPPC or *N*-P-SM. The monolayers also contained 1 mol% NBD-cholesterol as a fluorophore. After the initial compression to a lateral surface pressure of 1.5 mN/m, images of the monolayers were collected and digitized. The bars represent 100 μm, and all micrographs for one phospholipid type were obtained at the same magnification, but please note that the magnification for DPPC and *N*-P-SM differ.

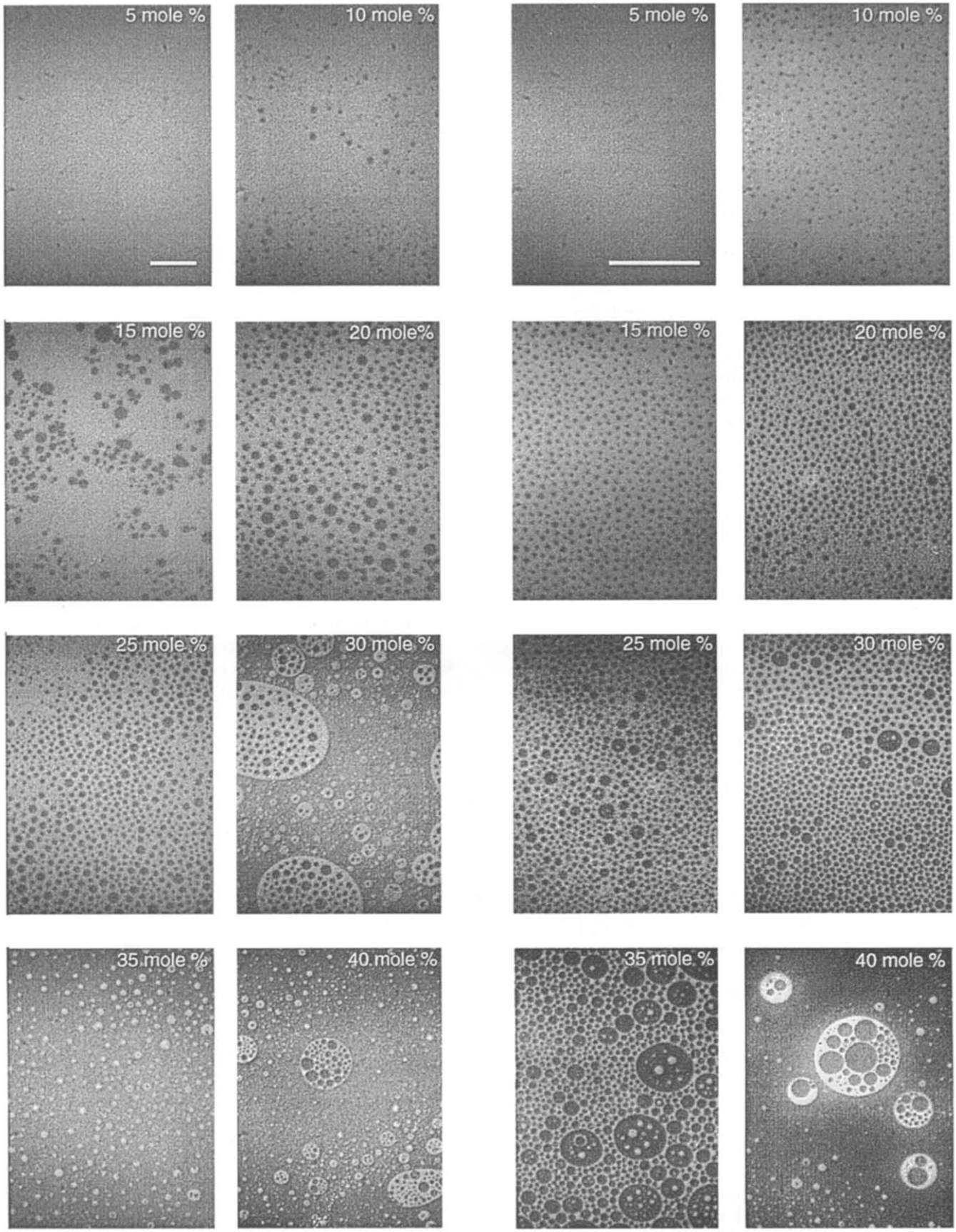
5 mole %
10 mole %
15 mole %
20 mole%
25 mole %
30 mole %
35 mole %
40 mole %
5 mole %
10 mole %
15 mole %
20 mole %
25 mole %
30 mole %
35 mole %
40 mole %
Cholesterol/DPPC
Cholesterol/N-P-SM

expanded domains, giving these a bright fluorescence, while the probes are largely excluded from more tightly packed liquid-condensed domains (giving them a darker appearance). This study has used NBD-cholesterol to study the formation of domains in DPPC and *N*-P-SM monolayers containing increasing amounts of cholesterol. At low cholesterol concentration (e.g., 5 mol%), both DPPC and *N*-P-SM mixed monolayers were uniformly fluorescent at 1.5 mN/m, indicating an apparently homogenous liquid-expanded phase without liquid-condensed dark domains (Fig. 1). However, with increasing cholesterol concentration, circular dark domains (liquid-condensed) begun to form (Fig. 1). In DPPC mixed monolayers at 10 and 15 mol% cholesterol, the liquid-condensed domains were unevenly distributed and appeared to aggregate into clusters, whereas the distribution pattern in *N*-P-SM monolayers at corresponding cholesterol concentrations was uniform. The liquid-condensed domains were observed to undergo Brownian motion in the plane of the monolayer. At 30 mol% cholesterol and above, the liquid-condensed domains appeared to have coalesced in DPPC mixed monolayers, whereas circular (drop-like) liquid-condensed domains persisted up to 35 mol% cholesterol in *N*-P-SM mixed monolayers. At these high cholesterol concentrations, the liquid-condensed domains invariably contained drop-like brightly fluorescent inclusions, which themselves included smaller dark drop-like liquid-condensed domains.

3.2. Quantitative characterization of liquid-condensed domains

In order to correlate the formation of dark liquid-condensed domains with the cholesterol concentration of the mixed monolayer, the area of the liquid-condensed domains was calculated. As shown in Fig. 2 (open symbols), the total area covered by the dark liquid-condensed domains increased with increasing cholesterol concentration. The area covered by the liquid-condensed domains increased similarly in DPPC and *N*-P-SM mixed monolayers up to about 25 mol%. At higher cholesterol concentrations, it appeared that DPPC monolayers were covered to a larger extent by liquid-condensed domains as compared to *N*-P-SM monolayers, possibly reflecting the coalescence of liquid-condensed domains at 30 mol% cholesterol in the DPPC system.

Although the total area covered by the liquid-condensed domains were similar in DPPC and *N*-P-SM monolayers (at least up to 25 mol% cholesterol), the domain characteristics were different. In DPPC mixed monolayers, the number of liquid-condensed domains per unit area was less than in *N*-P-SM mixed monolayers (Fig. 3, open symbols), but this was compensated for by a larger average area of the liquid-condensed domains in DPPC monolayers (Fig. 4, open symbols). With both phospholipid types, the number of liquid-condensed domains increased with increasing cholesterol concentration, with the increase being more

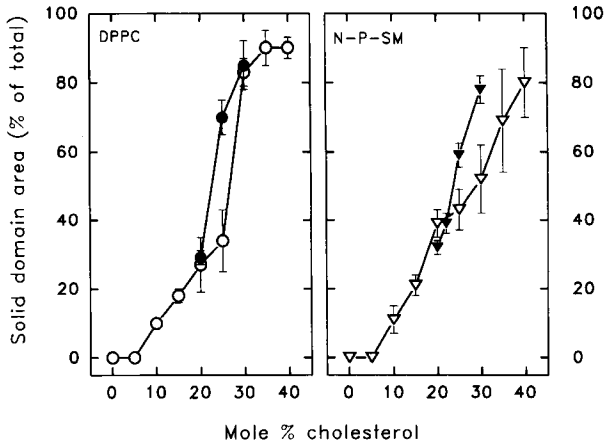

Fig. 2. Liquid-condensed domain area versus cholesterol concentration. The area of the liquid-condensed domains (see Fig. 1) over the total frame area (118500 μm^2) was analyzed from about 10 different micrographs from two separate and representative monolayers (compressed to 1.5 mN/m) for each cholesterol concentration and phospholipid type. The area is given as per cent of the total area, and the values are averages ± S.D. from the different frames. The open symbols represent solid domain areas during initial compression, whereas the filled symbols represent monolayers which were taken through a compression/expansion cycle (compression to 15 mN/m and expansion back to 1.5 mN/m, at which pressure calculations were performed).

marked in *N*-P-SM than in DPPC mixed monolayers (Fig. 3). With both systems, the average domain size also appeared to increase with increasing cholesterol concentration, although this trend was more consistent with *N*-P-SM mixed monolayers (Fig. 4). A look at the size distribution of the liquid-condensed domains at 20 mol% cholesterol revealed that these were more uniform in size in *N*-P-SM mixed monolayers than in DPPC monolayers (Fig. 5).

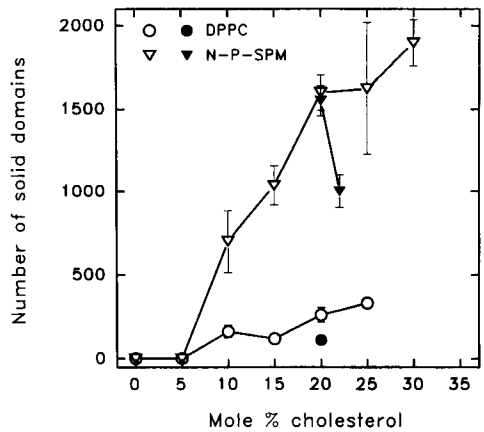

Fig. 3. Number of domains versus cholesterol concentration. The number of liquid-condensed domains were counted in a frame which had a size of 118500 μm^2. About ten frames from two separate monolayers were counted, and the values given are averages ± S.D. The open symbols represent the number of solid domains during initial compression, whereas the filled symbols represent solid domains in monolayers which were taken through a compression/expansion cycle.

3.3. Stability of domains

Subramaniam and McConnell [18] have previously reported a phenomenon of phase transformation in a cholesterol/dimyristoylphosphatidylcholine mixed monolayer system, the transformation of which is dependent on the lateral surface pressure. In this phase transformation, the lateral phase domains begin to display fluctuations in the shape of their one-dimensional line boundary [18]. In our system with cholesterol in DPPC or *N*-P-SM mixed monolayers, a similar surface pressure-dependent phase transformation was observed. The lateral surface pressure at which the line boundary between phases started to fluctuate and dissipate increased with increasing cholesterol concentration (Fig. 6), and was lower for the DPPC system as compared with the *N*-P-SM system. When the lateral surface pressure was reduced below the phase transformation pressure, the lateral segregation of liquid-condensed and liquid-expanded domains re-emerged.

The properties of the domains formed when a monolayer was subjected to a compression/expansion cycle varied with the concentration of cholesterol. At 20 mol% cholesterol in DPPC, the liquid-condensed domains were slightly larger in size after the compression/expansion cycle than before (Figs. 7A and 4, filled symbols) whereas their number had decreased (Fig. 3, filled symbols). With the *N*-P-SM system containing 20 mol% cholesterol, the properties of the liquid-condensed domains were similar before and after the compression/expansion cycle (Figs. 1 and 7E). At 25 mol% cholesterol (with both phospholipids), the compression/expansion cycle forced the liquid-condensed domains to coalesce (Fig. 7). The monolayer area covered by the liquid-condensed domains was larger after than before the compression/expansion cycle in those monolayers which had no significant liquid-condensed domain fusion below the phase transformation pressure (Fig. 2, filled symbols).

The phase fluctuations were not similar in DPPC and *N*-P-SM monolayers, especially if these were enriched in cholesterol. At 35 mol% cholesterol, the DPPC mixed

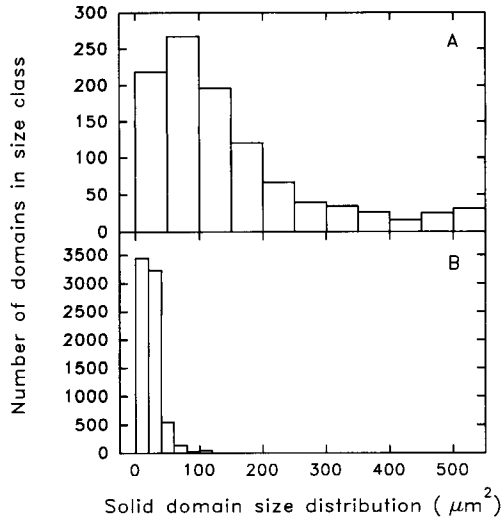

Fig. 5. Size distribution of liquid-condensed domains. The liquid-condensed domains of one representative frame (596450 μm^2) at 20 mol% cholesterol in either DPPC or *N*-P-SM were analyzed for their size distribution. With the DPPC mixed monolayer (panel A), size classes were selected to cover intervals of 50 μm^2 (with the rightmost column covering areas above 500 μm^2), whereas size classes were selected to cover intervals of 20 μm^2 in the *N*-P-SM mixed monolayer (panel B). The rightmost bar in panel B covers sizes larger than 100 μm^2.

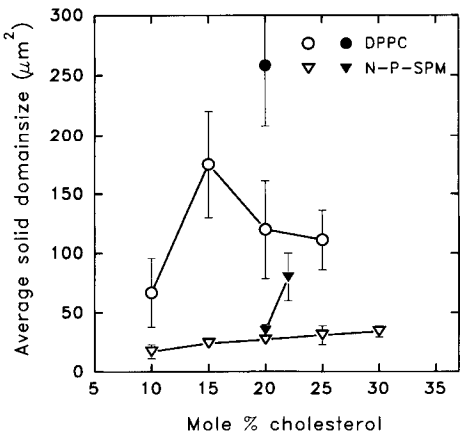

Fig. 4. Average liquid-condensed domain size versus cholesterol concentration. The average area of the liquid-condensed domains was calculated in 7 to 10 frames from two separate monolayers for each monolayer type. The values given are the mean values ± S.D. of the average domain sizes from each frame. The error bars therefore do not correctly indicate the domain size distribution in each individual frame. The open symbols represent the average solid domain size during initial compression, whereas the filled symbols represent solid domain sizes in monolayers which were taken through a compression/expansion cycle.

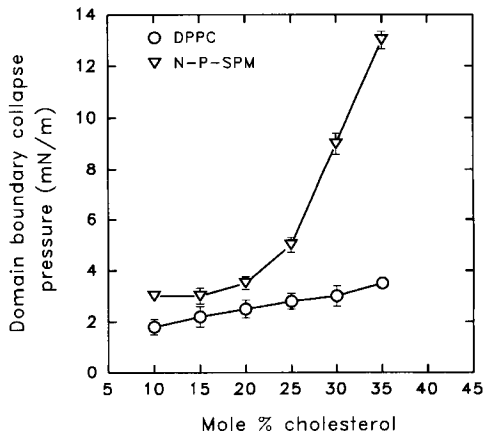

Fig. 6. Stability of lateral phase boundaries. The lateral surface pressure needed to destabilize the domain boundary in the mixed monolayers was determined in monolayers which were compressed slowly (3.4 $Å^2$/molecule, min). The lateral surface pressure at which the liquid-condensed/liquid-expanded domain boundary was distorted is indicated for mixed monolayers having cholesterol concentrations between 10 and 35 mol%. For *N*-P-SM monolayers having cholesterol concentrations at 30 mol% and above, it was further noted that at still higher surface pressure (filled triangle), the liquid-condensed domains started to coalesce (see also Fig. 8, panel B).

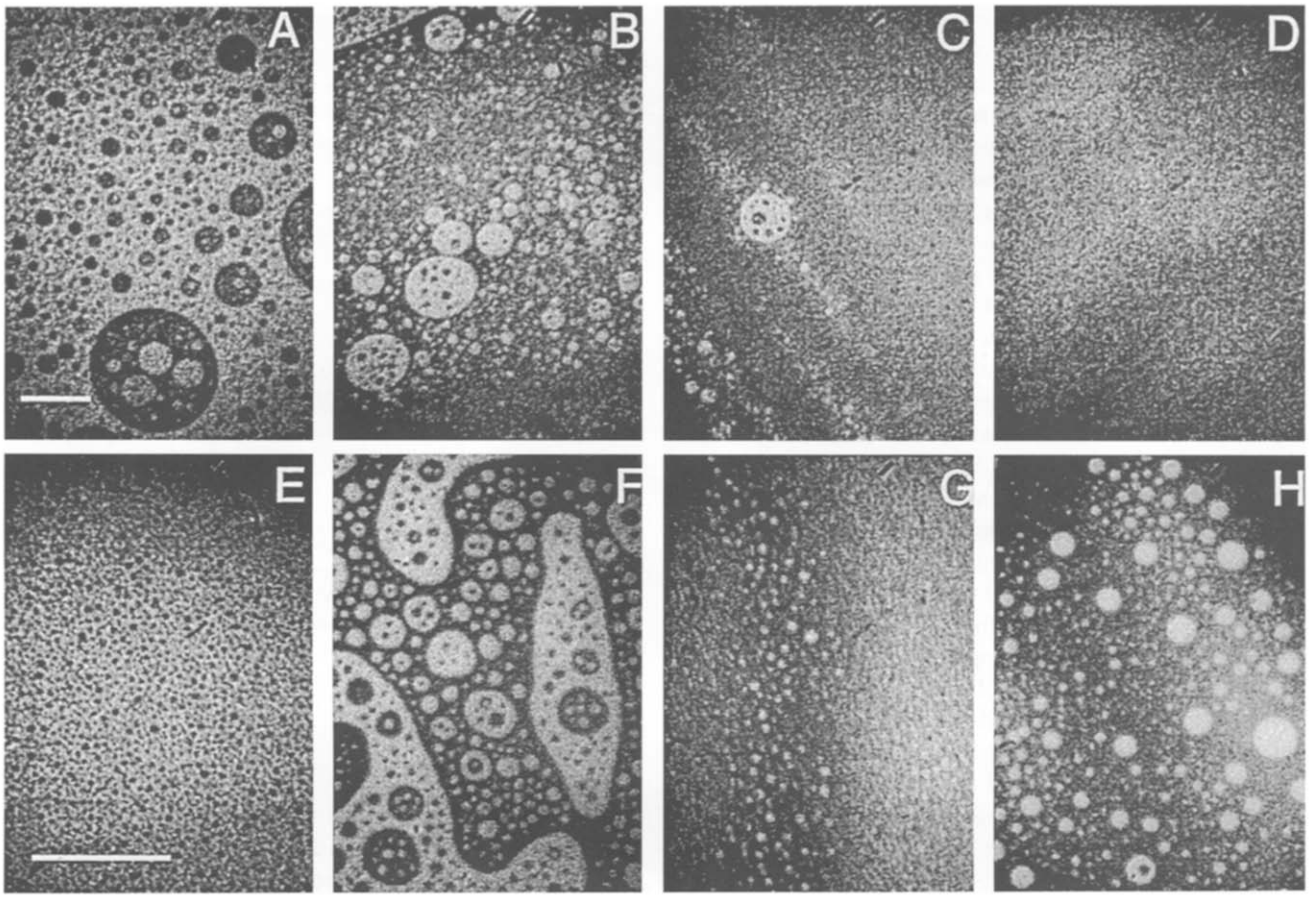

Fig. 7. Domain formation in mixed monolayers which have passed a compression/expansion cycle. Mixed monolayers containing increasing amounts of cholesterol (20 mol% in panel A and E; 25 mol% in B and F; 30 mol% in C and G; and 35 mol% in D and H) were prepared with either DPPC (the top row, panels A to D) or *N*-P-SM (the bottom row, panels E and H). The monolayers also contained 1 mol% NBD-cholesterol as a fluorophore. The monolayers were compressed to 15 mN/m, kept at this pressure for 30 s, and then expanded back to 1.5 mN/m. The bars in panels A and E represent 100 μm. All panels except E have the same magnification.

monolayers displayed a phase transformation which resulted in an apparently homogenous monolayer above the phase transformation pressure. When the surface pressure was lowered to 1.5 mN/m, the liquid-condensed domains had coalesced (Fig. 7D), and the liquid-expanded domains were very small in size (giving the micrograph in Fig. 7D

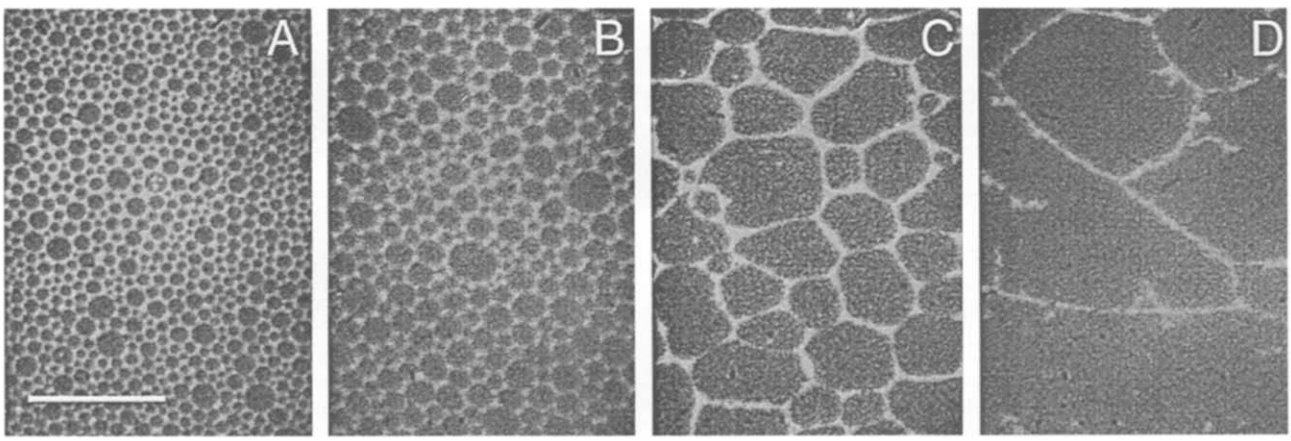

Fig. 8. Surface pressure dependent fusion of liquid-condensed domains. A *N*-P-SM mixed monolayer containing 35 mol% cholesterol was compressed at a speed not exceeding 3.4 Å^2/molecule, min. Panel A (during initial compression at 2 mN/m) shows the many drop-like liquid-condensed domains, which grew in size as the pressure increased to 9 mN/m (B). Further compression led to the fusion of liquid-condensed domains (12 mN/m, C). At still higher surface pressures, the string-like liquid-expanded domains narrowed significantly (20 mN/m, D). The scale bar represents 100 μm.

a homogeneously gray appearance). However, the *N*-P-SM mixed monolayer at 35 mol% cholesterol was very different. In this monolayer system, the liquid-condensed domains started to coalesce at the phase transformation pressure while the monolayer retained a sharp boundary line between probe-including and excluding phases. Details of the phase transformation behavior of a mixed *N*-P-SM monolayer containing 35 mol% cholesterol is shown in Fig. 8. When the monolayer was compressed from 2 mN/m (Fig. 8A) to 9 mN/m (at 5.4 Å^2/molecule, min; Fig. 8B), the liquid-condensed domains appeared to increase in size. When the pressure was increased further (to 12 mN/m, Fig. 8C), a marked fusion of liquid-condensed domains was observed. When the pressure was increased further (to 20 mN/m, Fig. 8D), the bright probe-including domains became narrower and irregular in shape. A relaxation of the mixed monolayer to 1.5 mN/m led to a swelling of the probe-including domains which with time (within a few min) developed into droplike bright inclusions within the liquid-condensed dark phase (as shown in Fig. 7H).

4. Discussion

It has previously been reported that binary mixtures of cholesterol and DPPC or dimyristoylphosphatidylcholine can form immiscible fluid phases at the air/water interface [18,19]. These immiscible fluid phases (liquid-condensed phases in a liquid-expanded phase, or vice versa) can conveniently be visualized by fluorescence microscopy, since suitable fluorescent lipid probes (e.g., NBD-phosphatidylcholine or NBD-cholesterol) partition selectively into the liquid-expanded phase and are largely excluded from liquid-condensed phases [16,17,21]. We have selected to use NBD-cholesterol instead of NBD-phosphatidylcholine, since NBD-cholesterol in our hands gives a slightly better contrast between probe-including and -excluding domains [20].

The present study has demonstrated *N*-P-SM mixed monolayers, in addition to the previously reported DPPC system [19], also show fluid phase immiscibility at the air/water interface in the presence of cholesterol. The existence of fluid phase immiscibility appeared to be a function of the transition temperature of the phospholipid examined and the experimental temperature, since di-17:0 phosphatidylcholine and phosphatidylcholine species with longer acyl chains (di-18:0 and di-20:0) do not form fluid phase immiscibility in the presence of cholesterol at 22° C (Slotte, unpublished observations). DPPC (T_c 41° C, [22]), *N*-P-SM (T_c 41° C; [23]), and phosphatidylcholines with shorter acyl chains (di-10:0 to di-15:0) form liquid-expanded and liquid-condensed lateral phases at ambient temperature when mixed with cholesterol (this study; and Slotte, unpublished observations). The formation of cholesterol-rich liquid-condensed domains in DPPC and *N*-P-SM mixed monolayers started at a cholesterol concentration higher than 5 mol%. At increasing cholesterol concentration, the area covered by cholesterol-rich liquid-condensed domains increased, as did the number of liquid-condensed domains. It has been shown that the free energy needed to create a critical nucleus for growth of the liquid-condensed phase can be reduced by increasing the temperature or surface charge density [24], by surface-active dyes [25], proteins [26] or cholesterol [27,28]. Based on our results, it is clear that cholesterol had a profound effect on the formation of liquid-condensed domains. Because the liquid-condensed domains formed at cholesterol concentrations up to 25 mol% (DPPC) or 35 mol% (*N*-P-SM) were circular (drop-like), it can be inferred that the molecules or the molecular aggregates in these domains were isotropic. Isotropy is expected to give circular domains because of the minimization of the solid/fluid interfacial free energy (i.e., line tension; [29]).

The monolayer interaction between cholesterol and *N*-P-SM resulted in the formation of significantly smaller liquid-condensed domains as compared with the corresponding cholesterol/DPPC system. The number of domains per unit area was, however, much larger for cholesterol/*N*-P-SM monolayers than for cholesterol/DPPC monolayers. This finding may imply that the free energy needed for the creation of critical nuclei for the growth of the cholesterol-rich phase was significantly lowered by a high-affinity attraction of cholesterol to *N*-P-SM, a phenomenon which was not observed in cholesterol/DPPC systems. The liquid-condensed domains formed in the presence of cholesterol were differently resistant to fusion in DPPC and *N*-P-SM mixed monolayers, if the monolayer had no history of precompression to a moderately high lateral surface pressure. In DPPC mixed monolayers, fused liquid-condensed domains begun to appear when the cholesterol concentration approached 30 mol%, whereas no large-scale fusion of liquid-condensed domains was seen in *N*-P-SM mixed monolayers until the cholesterol concentration reached 40 mol%. Since long range, dipole-induced repulsion prevent the liquid-condensed domains to fuse, these forces appear to be stronger in cholesterol/*N*-P-SM than in cholesterol/DPPC monolayers. This long range repulsion may in turn arise from differences in dipole properties of phosphatidylcholines and sphingomyelins [30,31], as well as from effects of the cholesterol/phospholipid association on the net dipole of *N*-P-SM and DPPC mixed monolayers.

The liquid-condensed domain properties are sensitive to compression of the mixed monolayer beyond a critical lateral surface pressure. McConnell and co-workers [18,19] have shown for a cholesterol/phosphatidylcholine mixed monolayer system that lateral phase boundary lines begin to fluctuate (shape transformation) and dissipate (creating an apparent one-phase system) at a certain lateral surface pressure. We observed that the lateral surface pressure at which the phase boundary lines dissipated was signifi-

cantly lower for cholesterol/DPPC monolayers than it was in mixed monolayers containing *N*-P-SM. With all cholesterol concentrations tested (10–35 mol%) in the DPPC monolayers, the phase boundary lines dissipated at the critical lateral surface pressure (which was between 1.8 and 3.7 mN/m). A similar phenomenon was seen with *N*-P-SM mixed monolayers at cholesterol concentrations up to 30 mol%. However, at 35 mol% cholesterol, the domain boundary line did not dissipate at this critical lateral surface pressure, but instead the cholesterol-rich liquid-condensed domains begun to fuse. The characteristic phase transformation pressure can also be obtained from an analysis of the force-area isotherm of binary monolayers containing cholesterol and a phospholipid, in that the compressibility function of the isotherm shows a discontinuity at a lateral surface pressure which is equivalent to the phase transformation pressure [32]. This phase transformation pressure appears not, however, to be related to the surface pressure at which the bulk phospholipids undergo their transition from a liquid-expanded to a liquid-condensed phase. The transition onset pressure (at 22° C in our laboratory) is about 4 mN/m for DPPC and 19 mN/m for *N*-P-SM (Slotte, unpublished observations).

When mixed monolayers were compressed beyond the critical lateral surface pressure at which phase transformations took place, or at which phase domain boundary lines dissipated, and then were allowed to expand below this same critical surface pressure, the lateral domain distribution was changed relative to the pre-transformation stage. This suggests that the domains formed during the initial compression were not equilibrium domain shapes. Usually (but not always) the phase transformations were reversible in the sense that upon compression lateral domains dissolved (sometimes giving an apparently homogenous monolayer phase), whereas these reformed (phase separation) when the monolayer was expanded below the critical surface pressure. The most significant finding was the pressure-induced fusion of the liquid-condensed domains in mixed monolayers containing 25 mol% cholesterol or more. This observation may relate to the results calculated by Snyder and Freire [33], in which they proposed that around 20 mol% cholesterol, there is a percolation process which connects cholesterol-rich lateral domains into a single cluster. This lateral connection of cholesterol-rich domains at about 20 mol% cholesterol was reported to be similar in DPPC and *N*-P-SM membranes [33].

In conclusion, the present study has added significant new information about lateral domain formation in mixed cholesterol/phospholipid monolayers. Although the domains observed in this study were seen at lateral surface pressure which was not even close to what can be expected in biological membranes, many other types of experiments still suggest that the distribution of cholesterol in model and biological membranes is heterogenous (i.e., that domains exists) even at high surface pressures [34–36]. The emphasis of this study has been on finding differences in how cholesterol interacts with phosphatidylcholine on one hand and with an acyl-chain comparable sphingomyelin on the other. The results regarding domain formation and stability indicate that the strength of association of cholesterol with sphingomyelin differ from that of DPPC. The more favorable association of cholesterol with sphingomyelin may derive from the amide-function in sphingomyelin, since it has been shown by us that cholesterol is more resistant to oxidation in monolayer membranes containing 3-deoxy-*N*-stearoylsphingomyelin than it is in 3-deoxy-*O*-stearoylsphingomyelin membranes [37]. Finally, it is worth noting that the direct visualization of lateral fluid domains in mixed monolayers at the air/water interface is an exciting experimental approach by which it may become possible to study the preferential association of cholesterol with phospholipids in ternary mixed monolayers (e.g., containing both phosphatidylcholine and sphingomyelin).

Acknowledgements

I thank Dr. Howard L. Brockman for helpful discussions. This study was supported in part by generous grants from the Sigrid Juselius Foundation, the Åbo Akademi University, and the Academy of Finland.

References

[1] Lange, Y. and Ramos, B.V. (1983) J. Biol. Chem. 258, 15130–15134.
[2] Lange, Y., Swaisgood, M.H., Ramos, B.V. and Steck, T.L. (1989) J. Biol. Chem. 264, 3786–3793.
[3] Lange, Y (1992) J. Lipid Res. 33, 315–321.
[4] Yeagle, P.L. (1985) Biochim. Biophys. Acta 822, 267–287.
[5] Bloch, K. (1991) in Biochemistry of Lipids, Lipoproteins and Membranes (Vance, D.E. and Vance, J., eds.), pp. 363–381, Elsevier.
[6] Lund-Katz, S., Laboda, H.M., McLean, L.R. and Phillips, M.C. (1988) Biochemistry 27, 3416–3423.
[7] Smaby, J.M., Brockman, H.L. and Brown, R.B. (1994) Biochemistry 33, 9135–42.
[8] Barenholz, Y. (1986) in Physiology of Membrane Fluidity (Shinitzky, M., ed.), pp. 131–173, CRC Press, Boca Raton.
[9] Finkelstein, A. (1987) Water Movement through Lipid Bilayers, Pores and Plasma Membranes. Theory and Practice, pp. 98–99, John Wiley and Sons, New York.
[10] Bittman, R. (1993) in Cholesterol in Model Membranes (Finegold, L.X., ed.), pp. 45–65, CRC Press, Boca Raton.
[11] Needham, D. and Nunn, D.S. (1990) Biophys. J. 58, 997–1009.
[12] Slotte, J.P. (1992) Biochemistry 31, 5472–5477.
[13] Mattjus, P. and Slotte, J.P. (1994) Chem. Phys. Lipids 71, 73–81.
[14] Von Tscharner, V. and McConnell, H.M. (1981) Biophys. J. 36, 409–419.
[15] Lösche, M., Sackmann, E. and Möhwald, H. (1983) Ber. Bunsenges. Chem. 87, 848–852.
[16] Peters, R. and Beck, K. (1983) Proc. Natl. Acad. Sci. USA 80, 7183–87.
[17] McConnell, H.M., Tamm, L.K. and Weis, R.M. (1984) Proc. Natl. Acad. Sci. USA 81, 3249–3253.

[18] Subramaniam, S. and McConnell, H.M. (1987) J. Phys. Chem. 91, 1715–1718.
[19] Rice, P.A. and McConnell, H.M. (1989) Proc. Natl. Acad. Sci. USA 86, 6554–6448.
[20] Slotte, J.P. and Mattjus, P. (1994) Biochim. Biophys. Acta 1254, 22–29.
[21] Nag, K. and Keough, K.M.W. (1993) Biophys. J. 65, 1919–1926.
[22] Chapman, D. (1973) in Form and Function of Phospholipids (Ansell, G.B., Hawthorne, J.N. and Dawson, R.M.C., eds.) pp. 117–143, Elsevier, Amsterdam.
[23] Barenholz, Y. and Thompson, T.E. (1980) Biochim. Biophys. Acta 604, 121–158.
[24] Helm, C.A., Laxhuber, L., Lösche, M. and Möhwald, H. (1986) Colloid Polym. Sci. 264, 46–55.
[25] Miller, A. and Möhwald, H. (1987) J. Chem. Phys. 86, 4258–65.
[26] Haas, H. and Möhwald, H. (1989) Thin Solid Films 180, 101–110.
[27] Weis, R.M. and McConnell, H.M. (1985) J. Phys. Chem. 89, 4453–59.
[28] Heckl, W.M., Cadenhead, D.A. and Möhwald, H. (1988) Langmuir 4, 1352–60.
[29] Keller, D.J., McConnell, H.M. and Moy, V.T. (1986) J. Phys. Chem. 90, 2311–2315.
[30] Shah, D.O. and Schulman, J.H. (1967) Lipids 2, 21–27.
[31] Smaby, J.M. and Brockman, H.L. (1990) Biophys. J. 58, 195–204.
[32] Seul, M. and Sammon, M.J. (1990) Phys. Rev. Lett. 64, 1903–1906.
[33] Snyder, B. and Freire, E. (1980) Proc. Natl. Acad. Sci. USA 77, 4055–4059.
[34] Rubinstein, J.L., Owicki, J.C. and McConnell, H.M. (1980) Biochemistry 19, 569–573.
[35] Schroeder, F., Jefferson, J.R., Kier, A.B., Knittel, J., Scallen, T.J., Wood, W.G. and Hapala, I. (1991) Proc. Soc. Exp. Biol. Med. 196, 235–252.
[36] Sankaram, M.B. and Thompson, T.E. (1991) Proc. Natl. Acad. Sci. USA 88, 8686–8690.
[37] Bittman, R., Kasireddy, C.K., Mattjus, P. and Slotte, J.P. (1994) Biochemistry 33, 11776–11781.